TU Delft

Delft University of Technology

Water hyacinths retain river plastics

Schreyers, Louise J.; van Emmerik, Tim H.M.; Bui, Thanh Khiet L.; Biermann, Lauren; Uijlenhoet, Remko; Nguyen, Hong Quan; Wallerstein, Nicholas; van der Ploeg, Martine

DOI
10.1016/j.envpol.2024.124118

Publication date
2024

Document Version
Final published version

Published in
Environmental Pollution

Citation (APA)
Schreyers, L. J., van Emmerik, T. H. M., Bui, T. K. L., Biermann, L., Uijlenhoet, R., Nguyen, H. Q., Wallerstein, N., & van der Ploeg, M. (2024). Water hyacinths retain river plastics. *Environmental Pollution*, *356*, Article 124118. https://doi.org/10.1016/j.envpol.2024.124118

Important note
To cite this publication, please use the final published version (if applicable).
Please check the document version above.

Copyright
Other than for strictly personal use, it is not permitted to download, forward or distribute the text or part of it, without the consent of the author(s) and/or copyright holder(s), unless the work is under an open content license such as Creative Commons.

Takedown policy
Please contact us and provide details if you believe this document breaches copyrights.
We will remove access to the work immediately and investigate your claim.

This work is downloaded from Delft University of Technology.
For technical reasons the number of authors shown on this cover page is limited to a maximum of 10.

Environmental Pollution 356 (2024) 124118

Contents lists available at ScienceDirect

Environmental Pollution

journal homepage: www.elsevier.com/locate/envpol

Water hyacinths retain river plastics☆

Louise J. Schreyers [a,*], Tim H.M. van Emmerik [a], Thanh-Khiet L. Bui [b], Lauren Biermann [c], Remko Uijlenhoet [a,d], Hong Quan Nguyen [b,e], Nicholas Wallerstein [a], Martine van der Ploeg [a]

[a] Hydrology and Environmental Hydraulics Group, Wageningen University and Research, Wageningen, The Netherlands
[b] Institute for Circular Economy Development, Vietnam National University, Ho Chi Minh City, Vietnam
[c] Faculty of Science and Engineering, University of Plymouth, Plymouth, United Kingdom
[d] Department of Water Management, Delft University of Technology, Delft, The Netherlands
[e] Center of Water Management and Climate Change, Institute for Environment and Resources, Vietnam National University, Ho Chi Minh City, Vietnam

ARTICLE INFO

Dataset link: https://doi.org/10.4121/21648152.v1, https://doi.org/10.4121/ec6776d7-1818-43a9-b88c-3d0fe26484c5.v1, https://doi.org/10.4121/ebb2d47e-e986-4dcf-9dc5-e8b069a81f94

Keywords:
Plants
Fluvial
Pollution
Macroplastics
Microplastics

ABSTRACT

Rivers represent one of the main conduits for the delivery of plastics to the sea, while also functioning as reservoirs for plastic retention. In tropical regions, rivers are exposed to both high levels of plastic pollution and invasion of water hyacinths. This aquatic plant forms dense patches at the river surface that drift due to winds and currents. Recent work suggests that water hyacinths play a crucial role in influencing plastic transport, by efficiently trapping the majority of surface plastic within their patches. However, a comprehensive understanding of the interaction between water hyacinths and plastics is still lacking. We hypothesize that the properties relevant to plastic transport change due to their trapping in water hyacinth patches. In particular, the length scale, defined as the characteristic size of the transported material, is a key property in understanding how materials move within rivers. Here, we show that water hyacinth patches trap on average 54%–77% of all observed surface plastics at the measurement site (Saigon river, Vietnam). Both temporally and spatially, we found that plastic and water hyacinth presence co-occur. The formation of plastic-plant aggregates carries significant implications for both clean-up and monitoring purposes, as these aggregates can be detected from space and need to be jointly removed. In addition, the length scale of trapped plastics (~4.0 m) was found to be forty times larger than that of open water plastics (~0.1 m). The implications of this increased length scale for plastic transport dynamics are yet to be fully understood, calling for further investigation into travel distances and trajectories. The effects of plastic trapping likely extend to other key properties of plastic-plant aggregates, such as effective buoyancy and mass. Given the prevalence of plant invasion and plastic pollution in rivers worldwide, this research offers valuable insights into the complex environmental challenges faced by numerous rivers.

1. Introduction

Rivers are important pathways for the delivery of land-based plastic waste into the oceans (Meijer et al., 2021). Tropical rivers are notable hotspots for plastic pollution, contributing to the majority of plastic emissions into the oceans. The fifty rivers with the highest plastic emissions into the ocean are all located in tropical regions (Meijer et al., 2021). Tropical rivers are also frequently affected by water hyacinths presence. Water hyacinths are a freely drifting invasive macrophyte species (Cook, 1996) that moves at the water surface (Kleinschroth et al., 2021), due to the combined action of currents and wind. Water hyacinths are considered widespread in 74 countries and have a more localized presence in another 42 countries (Rojas-Sandoval and Acedevo-Rodríguez, 2022). Janssen (2023) reported peak extents of water hyacinths of 14%–24% of river area at certain sections of the Saigon river (Vietnam). Co-occurrence of water hyacinth invasion and high levels of plastic pollution have been observed across the globe, in the Citarum river, Indonesia (Pritasari Arumdati, 2021), the Chao Praya river, Thailand (Pajai, 2022), the Sacramento-San Joaquin river delta, U.S. (Honig, 2020) and the Ozama river, Domenican Republic (The Ocean Cleanup, 2021).

The proliferation of water hyacinths creates dense patches at the river surface, resulting in the trapping of floating debris, including macroplastics (Schreyers et al., 2021a). Water hyacinth presence can in turn alter the vertical velocity profile and decrease surface flow velocities, thus affecting the flow dynamics of affected waterways (Abd-Elaal and Mahmoud, 2022). In addition, plastic transport is influenced by hydrological conditions such as river discharge (van Emmerik et al., 2022,

☆ This paper has been recommended for acceptance by Michael Bank.

* Corresponding author.
E-mail address: louise.schreyers@wur.nl (L.J. Schreyers).

https://doi.org/10.1016/j.envpol.2024.124118
Received 11 January 2024; Received in revised form 16 April 2024; Accepted 5 May 2024
Available online 16 May 2024
0269-7491/© 2024 The Author(s). Published by Elsevier Ltd. This is an open access article under the CC BY-NC license (http://creativecommons.org/licenses/by-nc/4.0/).

2023a; Vriend et al., 2023). These elements highlight the intricate interactions between river flow, plastic and water hyacinths.

Current understanding of plastic-water hyacinth interactions suggests that water hyacinths coverage influence river plastic transport dynamics. Water hyacinth presence is assumed to be the main factor that explains surface plastic transport seasonality in the Saigon river (van Emmerik et al., 2019). This is attributed to the effective trapping capacity of water hyacinth patches, as it was found that water hyacinths trap the majority of surface macroplastics (Schreyers et al., 2021a). However, the impact of water hyacinth patches on plastic transport has yet to be comprehensively investigated. The consistency of trapping and release dynamics of water hyacinths with respect to plastics over time remains unknown. Water hyacinth coverage exhibits significant temporal variability in multiple freshwater systems, both inter-annually and within a single year due to seasonality effects (Kleinschroth et al., 2021; Janssens et al., 2022). Previous studies have observed the trapping of surface macroplastics by water hyacinths (Lotcheris et al., 2024; Schreyers et al., 2021a,b), but these investigations were limited to short-term observations, spanning six weeks at most. As a result, these studies could not ascertain whether the co-occurrence between plastics and water hyacinth presence was merely coincidental nor investigate potential seasonality patterns. In addition, these studies did not thoroughly quantified water hyacinth coverage and plastic concentrations, limiting our ability to understand the nexus between transported plastic and drifting water hyacinth.

The trapping of plastics within water hyacinth patches is likely to alter the properties relevant to plastic transport (shape, dimensions, mass and buoyancy) (Valero et al., 2022), which now pertain to the plastic-plant aggregates rather than the plastic itself. Specifically, the characteristic length scale (hereafter referred to as 'length scale') can be hypothesized as a key variable in governing plastic transport in rivers, as this was found to be the case for other materials, such as large wood (Braudrick, 1997). The concept of length scale is important in understanding the dynamics of solid and soft materials and can also be useful for gaining insights into plastic transport dynamics. Different length scales can affect these floating materials buoyancy, mobility, their interaction with flow patterns, and potential for trapping or retention in different parts of the river environment. Our study focuses on the interactions between plastic and water hyacinths, due to its widespread presence in rivers heavily polluted with plastics. Our approach could be extended to encompass other drifting/floating elements found in river ecosystems, such as water lilies, alligator weeds, water ferns (Hassan and Nawchoo, 2020; Koncki and Aronson, 2015), and woody debris. There is preliminary evidence suggesting that these elements may also serve as carriers of surface macroplastics, as it was found to be the case for woody debris in mountainous rivers (Liro et al., 2022).

The goal of this paper is to provide insights on plastic-water hyacinth trapping mechanisms. Specifically, we have three objectives. First, we aim to characterize the extent of plastic trapping within water hyacinth patches. Second, we seek to quantify the change in length scale of transported plastics, as a result of their trapping in water hyacinths. Third, we explore the spatial and temporal co-occurrence patterns between plastics and water hyacinth presence. We conducted a year-long study in the Saigon river, Vietnam and collected 3544 Uncrewed Aerial Vehicle (UAV) images to estimate plastic concentrations, the ratio of trapped plastics over the total number of plastics and water hyacinth coverage at the river surface. In addition, we quantified for the first time plastic-plant aggregates characteristics, enabling us to estimate the relevant length scale of transported plastics. Gaining insights on plastic trapping in water hyacinth is relevant mainly for two reasons. First, interactions between water hyacinths and plastic are expected to become increasingly relevant globally. Indeed, plastic inputs into rivers are anticipated to increase and the rise in global temperatures is expected to expand both the coverage and geographical range of water hyacinths (Borrelle et al., 2020; Kleinschroth et al., 2021). Second, the formation of plastic-plant aggregates can represent an opportunity for joint monitoring (and clean-up) of such aggregates. Drifting plants like water hyacinths are visible from space, facilitating large-scale monitoring of these carriers of riverine plastic debris.

2. Data and methods

2.1. Study area

We measured plastic transport, water hyacinth abundance and plastic concentrations between December 12, 2020 and January 15, 2022 in the Saigon river, Vietnam (Fig. 1A). The Saigon river originates in Cambodia and flows into the Dau Tieng reservoir, approximately 120 km north of Ho Chi Minh City (HCMC) (Nguyen et al., 2020). South of the city, the Saigon river confluences with the Dong Nai river. The Saigon river is subject to a asymmetrical semi-diurnal tidal cycle. Because of

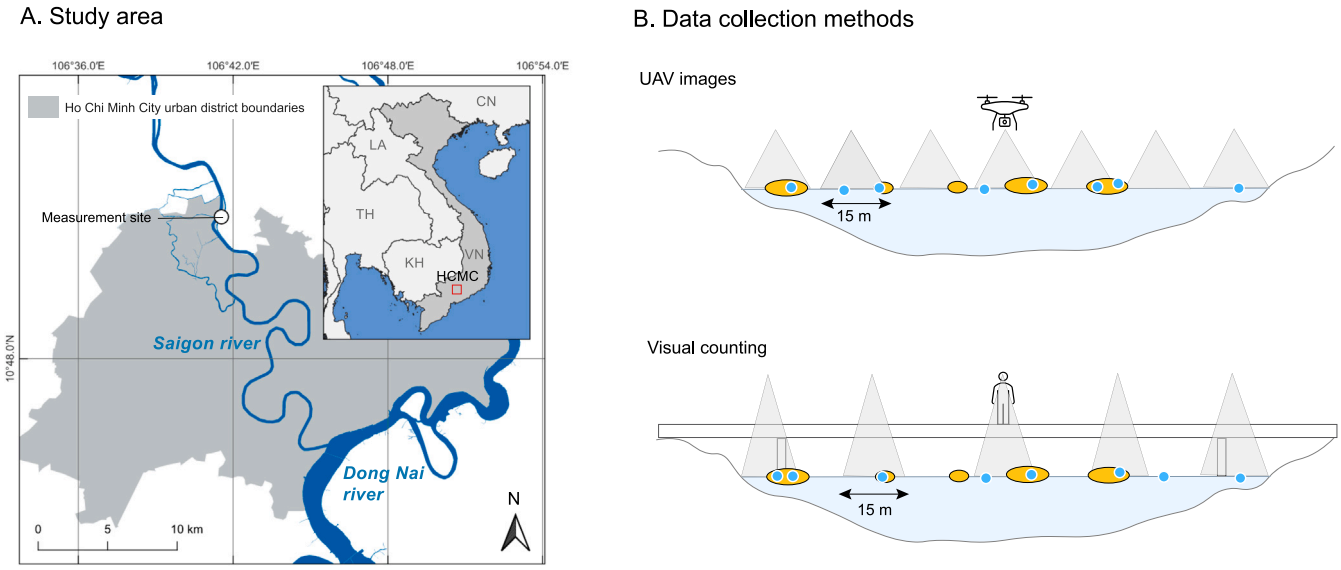

Fig. 1. A. Location map of the study area and measurement site in Ho Chi Minh City (HCMC), Vietnam. B. Overview of the two methods used for data collection: (1) UAV images (2) Visual counting from bridges. Visual counting was performed at nine points across the river width. Note that these are schematic representations and are not to scale.
Source: Adapted from van Emmerik et al. (2023b).

the tidal influence, the net river discharge is considered relatively low and subject to seasonal variations between the dry and wet seasons (monthly averages vary between −80 and + 320 m^3/s) (Camenen et al., 2021). In addition, the Saigon river is considered one of the most plastic polluted rivers in the world, with transport rates within the order of 10^4 #/h (van Calcar and van Emmerik, 2019). Water hyacinth invasions are also particularly severe in this river, with peak coverage reaching up to 14% of the river surface (Janssens et al., 2022).

This study focuses on surface macroplastic (size > 0.5 cm) concentration and transport, hereafter referred to as plastic for brevity. The measurement site is located north of the city (latitude: 10° 53′24.9"N; longitude: 106°41′31.5″E). Water hyacinth abundance and plastic concentrations were estimated using Uncrewed Aerial Vehicle (UAV) imagery analysis (Sections 2.2 and 2.3). Plastic transport was estimated using a visual counting method from bridges (Section 2.4) (Fig. 1B). The main variables used are summarized in Section 2.5.

2.2. Methods overview

A total of 3544 UAV images were taken across the river channel over 29 days, with a frequency of one to four flights per measurement day. More information on the UAV surveys is available in Appendix A (Extended Methods). A total of 900 visual counting observations were conducted over 39 days at one bridge.

Table S4 summarizes the measurement frequencies per month and the method applied at the measurement site. No data could be collected between July and October 2021, due to strict confinement in HCMC in response to the COVID-19 pandemic. In April 2021, no UAV flights were undertaken due to practical constraints.

2.3. Water hyacinth abundance

Water hyacinth patches were detected using UAV imagery analysis. We used a color filtering approach which enabled us to separate drifting vegetation content from other elements present at the river surface (e.g. water, banks, boats, wooden debris, surface plastics). This approach leverages the color characteristics of active vegetation in the visible range to distinguish it from other materials. To characterize water hyacinth abundance, 3544 images were processed. A few images (n = 18) were discarded because they were blurry, taken with a side-angle or due to the presence of boats which interfered with the water hyacinth detection. Image processing was done using the Open CV 4.5.4.60 library in Python 3.9.7. In addition to the color filtering, we performed morphological operations on the images, involving noise reduction and dilation to close small gaps. These operations and related parameters are detailed in Appendix A (Extended Methods). These operation parameters were defined by trial and error through visual inspection on an image subset, in order to maximize detection and minimize false positives as well as accurately detect the edges of the water hyacinth patches. A minimum threshold area (≥ 0.1 m^2) was also defined to filter out individual leaves and branches. Fig. 2 provides an example of water hyacinth detection for one UAV image. In Appendix B, Fig. S7 shows various examples of water hyacinth patches.

We quantify water hyacinth abundance in terms of coverage, patch count, average patch size and patch diameter (Table 1). Water hyacinth patch diameter [m] refers to the diameter of water hyacinth patches in the direction of the flow. We assume a circular shape of water hyacinth patches. This likely results in conservative estimates of water hyacinth diameters. Indeed, most patches are ellipsoidal in shape, with their major axis lying parallel to the flow direction.

2.4. Plastic concentrations

Plastic concentrations at the river surface were also quantified using UAV imagery analysis. The approach chosen is similar to the one described for water hyacinth detection in the previous section. The detection of surface plastics relied also on a color filtering operation, which filtered pixels of white and light gray color. This approach does not enable us to detect all surface plastics, which can be of varying color, opacity and transparency. However, our visual assessment on the entire dataset led to the conclusion that the majority (~ 70%–90%) of macroplastics were in this color range Fig. S7. This is consistent with previous studies that quantified macroplastic composition in the Saigon river and demonstrated the high proportion of plastics such as expanded polystyrene (food packaging, insulation foam), polystyrene (plastic cups and cutlery) and soft polyolefins (plastic bags and foils) (van Emmerik et al., 2019; Schreyers et al., 2021b). We found an accuracy score of 75% (Appendix A, Extended Methods), indicating an overall good detection of plastic. Additional details on the processing operations and their parameters are reported in Appendix A (Extended Methods). An example of plastic detection for one UAV image can be seen in Fig. 2. In Appendix B, Fig. S7 shows various examples of trapped and open water plastics.

2.5. Surface plastic transport

Plastic transport was estimated using the visual counting method, developed by González-Fernández and Hanke (2017) and now widely used in observational studies on macroplastic transport (van Calcar and van Emmerik, 2019; González-Fernández et al., 2021). All surface macroplastics (> 0.5 cm) were counted during a pre-defined time frame at each observation segment. Several observation segments were determined per measurement location, to account for the spatial variability in plastic transport across the river width (van Emmerik et al., 2018). Nine observation segments were selected at the measurement location (river width of 200 m), enabling us to cover 68% of the river width. At each observation segment, two types of observation were conducted: counting of *trapped* plastics, i.e.: plastics trapped in water hyacinth patches and counting of *open water* plastics, i.e.: plastics floating in the unobstructucted surface of the river. We detail in Appendix A (Extended Methods) how we estimated surface plastic transport [#/h] from the visual counting observations.

2.6. Main metrics of interest

The trapping ratio [-] (t_r) is calculated as the ratio between trapped plastics (N_t) and total plastics ($N_t + N_o$):

$$t_r = \frac{N_t}{N_t + N_o} \quad (1)$$

The trapping ratio was estimated using both the data on plastic transport and on plastic concentrations using UAV images. In both methods, open water and trapped plastics were distinguished.

We calculated three types of plastic concentrations: (i) **trapped** plastic concentrations, indicating the number of trapped plastics per unit area of water hyacinth coverage; (ii) **open water** plastic concentrations, indicating the number of open water plastics per unit area of open water. The open water area is calculated as the total river area minus the area covered by water hyacinths; (iii) **total surface** plastic concentrations, indicating the total number of plastics (both trapped and open water) per unit area of river surface, encompassing both open-water and water hyacinth-covered surfaces. All plastic concentrations were expressed as areal count concentrations [#/km^2].

We hereby define the 'length scale' as the characteristic longitudinal dimension of plastics and plastic-plant aggregates in the river flow direction. The length scale of trapped plastics (L_t) corresponds to the length scale of plastic-water hyacinth aggregates (excluding water hyacinths without plastics) (Section 2.2). The length scale of open water plastics (L_o) was estimated using size statistics derived from van Emmerik et al. (2019), who collected and measured 3022

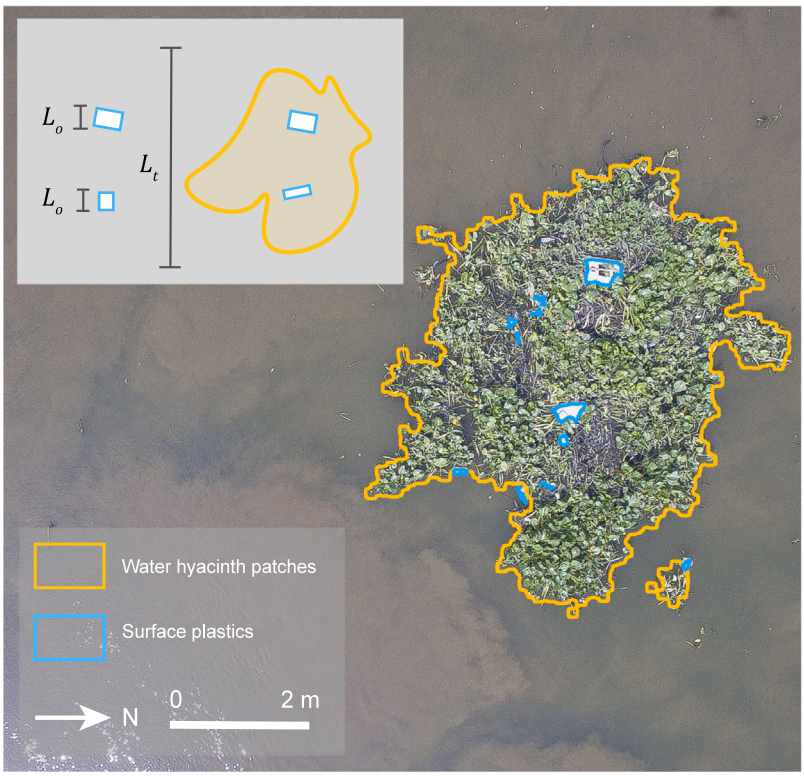

Fig. 2. Example of processed UAV image [from 6 November 2021] with surface plastics and water hyacinth patches identified. The insert panel schematically shows the estimation of the length scale of open water (L_o) and trapped items (L_t). Note that we assumed a circular shape of water hyacinth patches, thus the patch length is equal to the mean diameter. Also note that two trapped plastics are represented, meaning that the length scale for trapped plastics is calculated twice.

Table 1
Main variables of interest.

Variables	Description	Section and equation
Trapping ratio (t_r) [–]	Ratio of plastics found trapped in water hyacinth patches to total number of plastics	Section 2.6, Eq. (1)
Trapped plastic concentrations [#/km^2]	Number of trapped plastics over unit area of water hyacinth coverage	Section 2.6
Open water plastic concentrations [#/km^2]	Number of open water plastics over unit area of open-water river	Section 2.6
Total surface plastic concentrations [#/km^2]	Total number of plastics over river surface area	Section 2.6
Length scale of open water plastics (L_o) [m]	Size of open water plastics	Section 2.6
Length scale of trapped plastics (L_t) [m]	Length scale of plastic-water hyacinth aggregates (excluding water hyacinths without plastics)	Section 2.6
Average plastic length scale (L_p) [m]	Average of the combined distribution of length scale of trapped and open water plastics	Section 2.6, Eq. (2)
Water hyacinth relative coverage [–]	Ratio of water hyacinth coverage to river area	Section 2.3
Water hyacinth patches count [#]	Count of water hyacinth patches	Section 2.3
Water hyacinth patch size [m^2]	Average size of water hyacinth patches	Section 2.3
Water hyacinth patch diameter [m]	Assuming a circular shape of water hyacinth patches	Section 2.3
Plastic transport rate [#/h]	Number of plastics transported at the river surface	Section 2.5 and Eqs. (A.4) and (A.5), Appendix A

items over 45 measurement days at the Saigon river, between March and December 2018. The average plastic length of open water plastics was 0.1 m. For the probability distribution of plastic length scale, we used the entire population on items size. Fig. 2 shows a schematic representation of the length scale of both open water and trapped plastics.

In addition to the length scales of trapped and open water plastics, we also estimated the average plastic length scale (L_p) [m] as follows:

$$L_p = L_t \cdot t_r + L_o \cdot (1 - t_r) \quad (2)$$

This corresponds to the average of the combined distribution between the length scale of trapped and open water plastics.

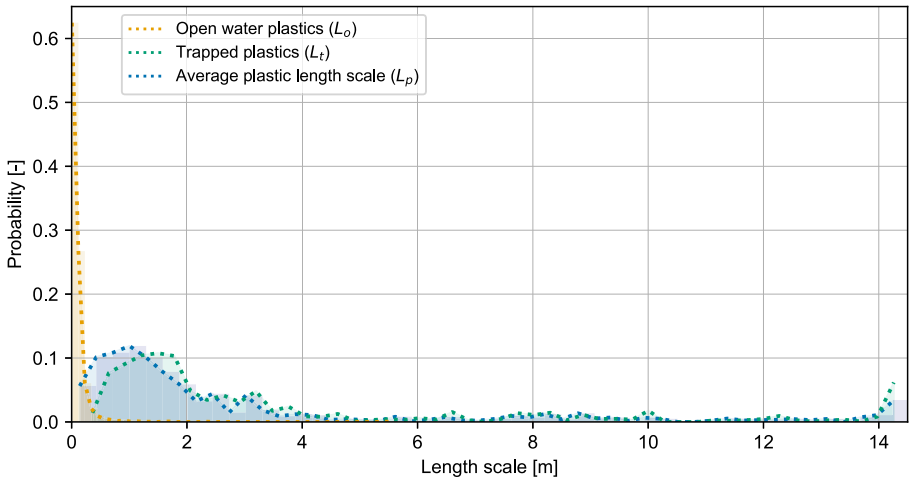

Fig. 3. Probability density of plastic length scale for open water plastics, trapped plastics and all plastics combined (average plastic length scale).

3. Results

3.1. Water hyacinths as effective plastic accumulators

On average, water hyacinth patches trap between 54% and 77% of plastic, depending on the monitoring method used. A higher trapping ratio (77%) was found using UAV images, and lower (54%) using visual counting, a likely results of the limited visibility within water hyacinth patches using visual counting. Trapping ratios vary importantly throughout the monitored period, with daily averages ranging from 41% to 98% for UAV images and 0% and 90% for visual counting. Water hyacinth patches cover only 6% of the river surface on average, thus indicating that patches trap more plastic than could be expected based on their relative coverage of the river surface (Fig. S8). As a result, concentrations of trapped plastics are almost 32 times higher than the concentrations of open water plastics, with $3.4 \cdot 10^5$ #/km^2 and $1.1 \cdot 10^4$ #/km^2, respectively (Table S5A).

Large water hyacinth patches trap proportionally more plastics than smaller ones. Water hyacinth patches above 5 m in length represent only 5% of patches but trap as much as 18% of plastics (Table S5B). We did not find a clear proportional relationship between water hyacinth relative coverage and trapping ratio. However, higher water hyacinth coverage usually corresponds to a higher trapping ratio and plastic concentrations (Fig. S8 and Table S5B). For water hyacinth coverage that exceeds 31% of the river surface, trapping ratios are all above 0.5.

3.2. Trapping in water hyacinths increases the relevant length scale for plastic transport

In the absence of trapping in water hyacinth patches, the length scale of plastic is determined solely by its own dimensions. For trapped plastics, the dimensions of plastic-water hyacinth aggregates determine the relevant length scale. Open water plastics have an average length scale of 0.1 m and range from 0.001 m to 5.6 m. The length scale of trapped plastics averages 4.0 m, representing a forty-fold increase compared to open water plastics (Table S5B and Fig. 3). Length scales exceeding one meter are extremely rare for open water plastics (less than 0.5%). However, in the presence of water hyacinths, we found that 89% of trapped plastics have a length scale above one meter, and 52% above two meters. Smaller plastic length scales are much less prevalent, with less than 1% of trapped plastics below 0.5 meter, compared to 98% of open water plastics falling within this range.

Combining both open water and trapped plastics, the resulting average plastic length scale is 3.1 m, close to thirty times more than for open water items (0.1 m). The average plastic length scale varies by as much as two orders of magnitude, from an average of 0.1 m for open water plastics to more than 10.0 m for trapped ones (Table S5B and Fig. 3). The average plastic length scale distribution closely follows that of trapped plastics (Fig. 3).

This highlights the dominant role of plastic-water hyacinth aggregates in determining the relevant length scale for plastic transport. Average plastic length scales are much higher than expected for a system without water hyacinths, due to the relative large diameter of water hyacinth patches. However, the overall mean patch diameter of water hyacinth is 1.8 m (mean patch size of 2.6 m^2), well below the average length scale of trapped plastics (4.0 m) (p-value < 0.05). This discrepancy reflects the fact that large water hyacinth patches have a higher trapping efficiency than smaller ones (Table S5B).

3.3. Plastic-plant aggregates co-occur over time

Comparing between UAV images with and with very limited water hyacinth coverage (Table 2) shows that the vast majority of observed plastics (95%) are detected in images with water hyacinth. In images with very limited water hyacinth presence (less than 0.01 relative coverage), the total surface plastic concentration and average plastic length scale are mainly governed by the plastic concentration and the length scale of open water plastics. Interestingly, the open water plastic concentrations increased in images with water hyacinth coverage compared to images with very limited water hyacinth coverage; whereas trapped plastic concentrations decreased. In the Discussion section we provide an hypothesis to explain this.

A seasonality pattern emerges, with higher hyacinth coverage, plastic transport and concentrations during the dry season compared to the wet season. However, due to limited observations during the wet season (Table S4), we cannot determine with certainty the significance of the observed differences. We observed higher average plastic transport rates during the dry season compared to the wet season (p-value = 0.01). During the dry season, the mean plastic transport rate amounts to $1.4 \cdot 10^4$ #/h, while during the wet season it decreases to $8.3 \cdot 10^3$ #/h (Table S6). These higher plastic transport rates observed during the dry season contradict the hydrological seasonality observed in the Saigon river, which is characterized by increased rainfall and discharge during the wet months (Appendix D, Fig. S9). This challenges a main working hypothesis in plastic transport studies, which postulates that higher river discharge would result in greater transport rates. Plastic concentrations also show a seasonal pattern, with significantly higher averages recorded during the dry months compared to the wet season. Although hyacinth coverage appears slightly larger during the dry season compared to the wet season, the values are not statistically significantly different (Table S6).

Table 2
Plastic-water hyacinth statistics with and without water hyacinth presence. All values were tested for statistically significant differences between water hyacinth and very limited water hyacinth presence, using a Kruskal–Wallis test and were all found significant (p-values < 0.05). Dry and wet refer to the dry and wet seasons.

	Water hyacinth presence (> 0.01 relative coverage)	Very limited water hyacinth presence (≤ 0.01 relative coverage)
UAV images [#]	1273	2281
UAV images (dry) [#]	857	1552
UAV images (wet) [#]	461	729
Total surface plastic concentration (open water & trapped) [#/km^2]	4.2 ·10^4	5.0 ·10^3
Open water plastic concentration [#/km^2]	1.4 ·10^4	3.4 ·10^3
Trapped plastic concentration [#/km^2]	2.6 ·10^5	5.0 ·10^5
Trapping ratio [–]	0.8	0.4
Plastic distribution [%]	95	5
Water hyacinth patch diameter [m]	2.2	0.6
Average plastic length scale [m]	3.2	0.3

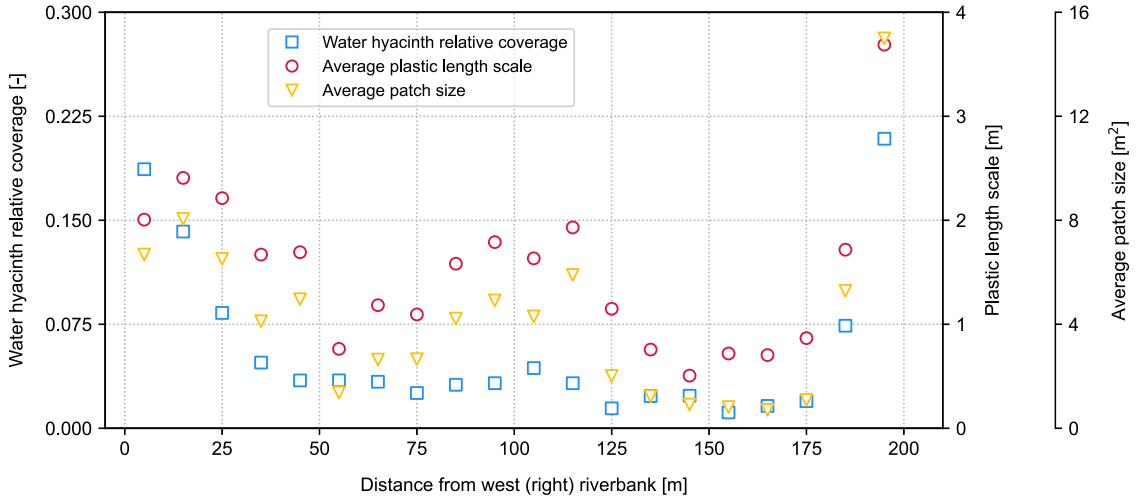

Fig. 4. Water hyacinth coverage, plastic length scale and average patch size at the river cross-section, as a function of distance from the riverbank.

3.4. Water hyacinth patches create a buffer zone along the channel sides, where most plastics are trapped

Spatially, water hyacinth patches predominantly occupy the channel's sides, establishing a buffer zone between the active river channel and the riverbanks (Fig. 4). In the initial 10 meters of each channel side, 71% of the UAV images displays more than 10% water hyacinth coverage (relative water hyacinth coverage > 0.1) on the surface area. In contrast, in other sections of the channel cross-section, images with over 10% water hyacinth coverage drop to 11%. The distribution of relative water hyacinth coverage forms a distinctive 'W' shape, with higher coverage on the sides and a smaller peak in the middle of the channel. Patch sizes follow a similar 'W' shape, with a few larger patches at positions 95 m and 115 m in the channel's middle (Fig. 4). As expected, the distribution of the average plastic length scale mirrors this pattern, primarily because its calculation incorporates the average patch size. Total surface plastic concentrations also show a similar distribution pattern and have highly significant correlations with the spatial distribution of water hyacinth coverage, patch size, and average plastic length scale (p-values < 0.01 and Spearman's $\rho \geq 0.6$).

4. Discussion and outlook

4.1. Plastic-water hyacinth interactions and their trajectories in rivers

We find that water hyacinth patches trap the majority of plastics at our measurement site in the Saigon river (54% to 77%, depending on the method used). Recent research by Janssen (2023) reveals that, despite a longitudinal decrease in water hyacinth patch size and coverage along the Saigon river (over a section spanning approximately 40 km), the trapping ratios remain consistently high between different measurement sites, ranging between 60% and 70% on average. This indicates that water hyacinth patches continue to be effective trappers throughout the course of the river.

The trajectories of drifting water hyacinth patches at the river surface likely differ from those of open water plastics due to differences in size, shape, density and mass. Transport factors such as wind, flow velocities and water levels affect water hyacinth patches and open water plastics differently. Our observations indicate that patches efficiently collect plastics along their trajectories, although we do not quantify the velocities of open water plastics and water hyacinth patches. Further studies investigating the trajectories of water hyacinth and open water plastics in relation to hydrological factors would contribute to understanding their transport and retention dynamics.

4.2. Plastic trapping in water hyacinths may lead to a re-distribution of plastic within the river system

We observe that the presence of water hyacinths co-occurs with increased total surface plastic concentrations. The total surface plastic concentrations and open water plastic concentrations both increased in the presence of water hyacinths. An opposite trend is observed for trapped plastic concentrations, with higher concentrations when water hyacinth coverage is very low (<0.01 of relative coverage). In such cases, trapped plastic concentrations are high due to the limited size and area covered by water hyacinth patches. As water

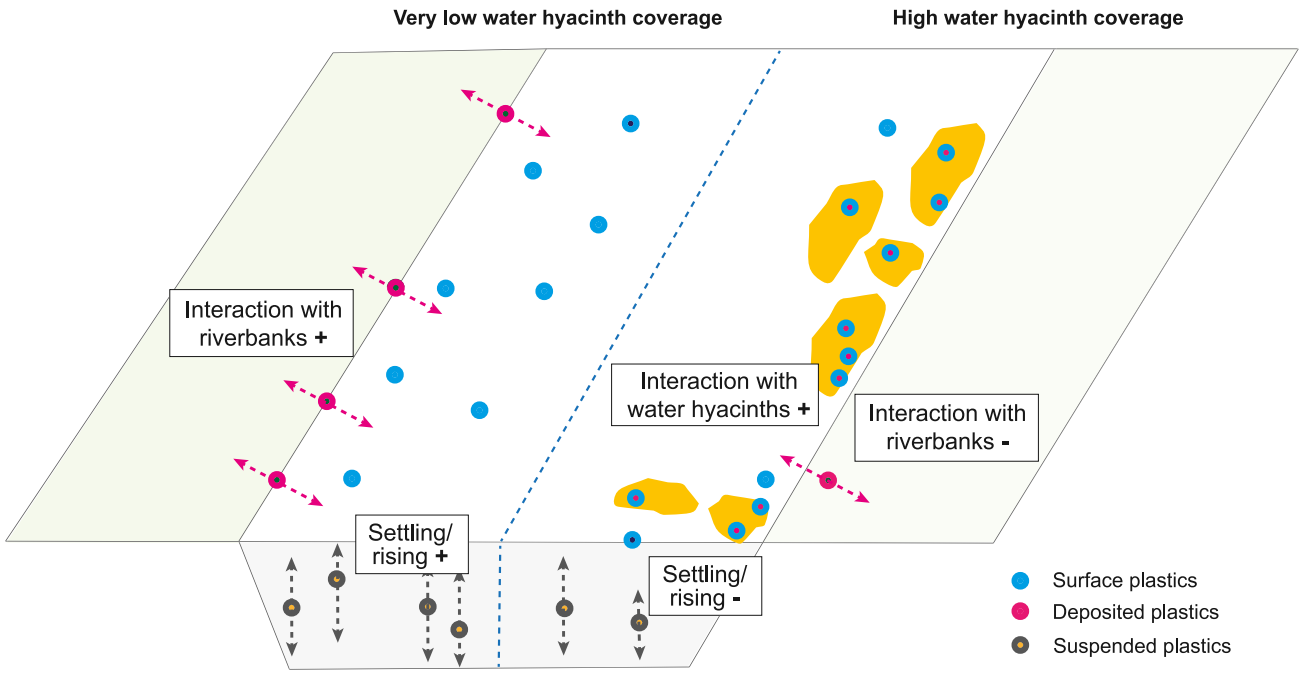

Fig. 5. Cross-sectional view of plastic-water hyacinth interactions. Pluses and minuses signs represent an increase/decrease in expected quantities in reference to a situation with very low water hyacinth coverage.

hyacinth coverage increases, trapped plastic concentrations decrease, but a larger number of plastics become trapped.

We hypothesize that the observed increase in total surface plastic concentrations is due to a redistribution of plastics within the river, caused by the water hyacinth presence (Fig. 5). Water hyacinths modify the transport characteristics of trapped plastics, including effective buoyancy. The trapping of neutrally and negatively buoyant plastics likely results in both a decrease in suspended (i.e.: located below the water surface) plastic concentrations and increase in total surface plastic concentrations. Negatively and neutrally buoyant plastics, such as bags and soft fragments, tend to sink below the surface due to changes in turbulence (Acha et al., 2003; Ballent et al., 2012). In rivers where water hyacinths are abundant, such as the Saigon river, these plastics are found in large quantities at the surface. Soft polyolefin plastics, including bags and soft fragments, represent 31% of all plastics found at the surface of the Saigon river (van Emmerik et al., 2019). Their trapping in water hyacinth patches may impede their sinking below the surface, contributing to the overall increase in total surface plastic concentrations in water hyacinth-affected areas. Other factors may explain the higher total surface plastic concentrations observed in the presence of water hyacinths. For instance, lower river discharge during the dry season could facilitate the retention of plastic and water hyacinths within the river. This is in line with our observations, which highlight higher plastic concentrations, transport rates and water hyacinth coverage in the dry season compared to the wet season.

Additionally, water hyacinths act as a buffer between the channel and the riverbanks, reducing the interactions with the banks. This is supported by the findings of Lotcheris et al. (2024), who observed that only 18% of the (temporarily) stopped plastics were deposited on the riverbanks, while the majority remained trapped within the water hyacinths in the river channel. Among the plastics that did reach the banks, only 30% were found in patches. These results suggest that the deposition of water hyacinth patches on riverbanks is unlikely.

4.3. Targeting clean-up efforts and monitoring on water hyacinth patches

Plastic trapping in water hyacinths leads to the formation of plastic-plant aggregates, which carries significant implications for both clean-up and monitoring purposes. Clean-up structures such as booms or vessels need to be designed to accommodate both the mass and dimensions of plastic and the water hyacinth in which it is trapped; a consideration that is currently not taken into account in existing designs (Helinski et al., 2021). In the Saigon river, plastic accounted for 6% of the total wet mass of collected debris (van Emmerik et al., 2019). The remaining majority consisted of organic material, particularly water hyacinths. Water hyacinths dry mass averages between 7.5 and 15 kg/m^2, whereas plastic dry mass is only 0.09 kg/# on average (van Emmerik et al., 2019; Reddy and Sutton, 1984). Consequently, clean-up actions targeting river plastics in water hyacinth affected areas require handling of substantial higher masses of plastic-plant aggregates compared to open water plastic only.

In rivers unaffected by water hyacinths, other types of vegetation are also found to form aggregations with plastics. For example, in the Seine river, debris collected by booms consisted of only 1% to 5% plastics, with the remaining 92% to 99% being mainly vegetative material (Gasperi et al., 2014). The presence of plastic-plant aggregates also affects the handling, sorting and removal of the collected debris (Hurley et al., 2023). This likely necessitates additional resources, infrastructure, and time to effectively remove the aggregated debris and isolate the plastic component.

We observed a strong relationship between water hyacinth coverage and plastic concentrations, suggesting that water hyacinth coverage could also serve as a convenient proxy indicator for plastic concentrations in polluted rivers. Both spatially and temporally, water hyacinth coverage and plastic concentrations co-occur. This suggests that monitoring and clean-up efforts could be directed towards periods of water hyacinth invasions (dry months) and areas where they are prevalent, particularly along the sides of the river channel.

Monitoring water hyacinth coverage can be efficiently achieved using satellite imagery, thanks to their distinctive spectral characteristics (Kleinschroth et al., 2021; Schreyers et al., 2022). This presents an opportunity to potentially upscale river plastic monitoring efforts. Our study found that larger water hyacinth patches are more effective at trapping surface plastics than smaller ones, suggesting a potential focus on the removal of large plastic-plant aggregates. For example, patches exceeding one meter in diameter trap over two-thirds of surface macroplastics. This facilitates the use of water hyacinth patches as a

proxy indicator for plastic concentrations, as detecting relatively large patches is more feasible compared to smaller ones. The later may fall below the detection range of currently available satellite sensors, such as Worldview (1.2–1.8 m/pixel).

4.4. Limitations and outlook

While our study provides valuable insights into the interactions between water hyacinths and plastic in rivers, several limitations should be acknowledged. Firstly, our measurements were confined to a single site in the Saigon river. This limits the applicability of our findings to other areas. However, recent evidence shows that the trapping mechanisms observed at our study site are common throughout the entire Saigon river (Janssen, 2023). To ensure the general applicability of our findings, further studies across different rivers beyond the Saigon River are needed. Secondly, the quantification of plastic trapping within water hyacinths presents some uncertainties. Water hyacinth leaves and stems can potentially obscure parts or entire pieces of plastics, thus limiting the detection through both imagery analysis and visual observations of trapped plastics. Conversely, the contrasting background provided by water hyacinth patches may enhance the visibility of trapped plastics compared to that of open water plastics. In addition, visual observations conducted from bridges are likely more uncertain in estimating trapping ratios when compared to UAV imagery, primarily due to the fact that observers tally moving plastics. Overall, the uncertainty in detecting trapped plastics is difficult to quantify. Cross-validation of our observations is hindered by the lack of simultaneous data collection, making it difficult to directly compare results obtained at different times. Future studies should aim to address these limitations to provide a more comprehensive understanding of plastic trapping in water hyacinth patches. Thirdly, the quantification of the length scale of water hyacinths and trapped plastics is also uncertain. We assumed a circular shape of water hyacinth patches, which likely results in an underestimation of patch diameter, since most patches were ellipsoid in shape. Consequently, this assumption may lead to an underestimation of the length scale of trapped plastics and water hyacinth patch diameters. Using other approaches to estimate patch diameter could reduce this uncertainty. Lastly, another limitation concerns the seasonal variability, as the statistical differences between the dry and wet seasons were not significant for some of the investigated variables. This was notably the case for the variables related to water hyacinth abundance, such as water hyacinth coverage and average patch size. This is likely the result of the limited number of observations during the wet months (Table S4). Indeed, recent studies on water hyacinth coverage over the Saigon river consistently reported lower coverage over the wet months (Janssens et al., 2022) throughout several years of observations, thus demonstrating the seasonality in water hyacinth coverage.

One critical aspect that requires further investigation is the time-scale of trapping and release of plastics within water hyacinth patches. We have observed that plastic-plant aggregates are highly dynamic, with patches trapping and releasing plastics in a matter of minutes, and temporarily pausing along the sides of the river (videos 1 and 2, Appendix C). However, the precise mechanisms and rates of trapping and subsequent release have not been quantified. These temporal dynamics have implications for both the overall distribution of plastics within river compartments and plastic transport dynamics. Methods such as UAV images and visual counting offer valuable but limited snapshots (in both space and time) of water hyacinth coverage and trapping processes. By leveraging the capabilities of video analysis, we have the potential to gain deeper insights into the intricate interactions between water hyacinth and plastics, thereby enhancing our understanding of their complex transport dynamics in rivers.

In addition to understanding trapping mechanisms, it is also crucial to investigate the trajectories of both water hyacinths and open water plastics. Conducting GPS tracker experiments offers a valuable opportunity to gain insights into the movement patterns of these materials. Such experiments can provide detailed information on various aspects, including velocity, traveled distance, pausing and stopping periods, and position within the river channel (Ledieu et al., 2022; Tramoy et al., 2020).

5. Conclusions

Water hyacinth functions as a major aggregator for surface plastics in rivers. Plastic concentrations in water hyacinths were found to be 32 times higher than those of open water plastics at the river surface and between 54% and 77% of the total transported plastics were trapped by water hyacinth patches. In addition, we found that large water hyacinth patches are more efficient trappers than smaller ones. These plant-plastic dynamics are not unique to our observation location, as similar trends were found at other locations in the Saigon river. This suggests that the results are transferable to other sites within the river, and to other fluvial systems invaded by water hyacinths. Trapping of plastics within water hyacinth patches increases by a factor of forty plastic length scale for plastic transport, from 0.1 m on average in the absence of water hyacinths to 4.0 m for plastic-plants aggregates. Trapping in water hyacinths may also modify other properties relevant for plastic transport, such as buoyancy and mass. Although the implications for transport dynamics remain unresolved, preliminary evidence suggests that plastic-plant aggregates are often associated with the (momentary) stopping of plastic trajectories on the sides of the river channel.

Our research revels that plastic and water hyacinth presence co-occur in time and space. We identified a seasonality trend, with larger water hyacinth coverage and higher plastic concentrations and transport rates in the dry season (Dec.-Apr.) compared to the wet season (May-Nov.). Additionally, water hyacinth patch accumulates mainly along the edges of rivers, where the highest plastic concentrations are found too. This holds implications for both monitoring and clean-up efforts, which could specifically target hotspots of plastic-plant aggregates.

Understanding the time-scale of trapping and release, the influence of changing hydraulic properties, and the different trajectories of water hyacinths and open water plastics will advance our knowledge and help to inform better targeted management. Addressing these research gaps is essential for developing comprehensive strategies to mitigate the impact of plastic pollution. Our study focused on one site at the Saigon river in Vietnam. Further research is required to assess the relevance and applicability of our findings to the entire Saigon river system, as well as to other rivers.

Water hyacinth patches are identified as significant temporary and mobile aggregators of plastics. The mechanisms driving water hyacinth drifting and temporary stopping at the river surface also influence the propagation of plastics in rivers. Conceptually, this suggests a potential fundamental modification of plastic transport dynamics due to the presence of water hyacinths.

CRediT authorship contribution statement

Louise J. Schreyers: Writing – original draft, Visualization, Validation, Methodology, Investigation, Formal analysis, Data curation, Conceptualization. **Tim H.M. van Emmerik:** Writing – review & editing, Supervision, Methodology, Funding acquisition, Conceptualization. **Thanh-Khiet L. Bui:** Writing – review & editing, Investigation. **Lauren Biermann:** Writing – review & editing, Funding acquisition. **Remko Uijlenhoet:** Writing – review & editing, Supervision. **Hong Quan Nguyen:** Writing – review & editing. **Nicholas Wallerstein:** Writing – review & editing, Supervision. **Martine van der Ploeg:** Writing – review & editing, Supervision.

Declaration of competing interest

The authors declare that they have no known competing financial interests or personal relationships that could have appeared to influence the work reported in this paper.

Data availability

The UAV images used in this manuscript are available at doi: https://doi.org/10.4121/21648152.v1. The UAV videos are available at https://doi.org/10.4121/ec6776d7-1818-43a9-b88c-3d0fe26484c5.v1. Other datasets used in this manuscript are available at: https://doi.org/10.4121/ebb2d47e-e986-4dcf-9dc5-e8b069a81f94.

Acknowledgments

The work of LS was supported by the Discovery Element of the European Space Agency's Basic Activities (ESA contract no. 4000132682/20/NL/GLC). The work of TvE was supported by the Veni Research Program, the River Plastic Monitoring Project with project number 18211, which was (partly) financed by the Dutch Research Council (NWO).

Appendix A. Extended methods

UAV surveys

Each UAV flight consisted of two overpasses across the Saigon river, resulting in 41 to 65 images taken per flight. Depending on the number of images taken per flight, the total river width monitored ranged between 226 m and 358 m. Considering that the river width at the measurement site is approximately 200 m, this indicates that there was an overlap of UAV images ranging from 13% to 79%. UAV surveys were performed at a constant elevation of approximately 10 m above the water level. Each image covered approximately 165 m^2 of the river surface (15 m of width by 11 m of length). One UAV flight thus captured between 6765 and 10,725 m^2 of the river surface at the measurement site.

We used the DJI Phantom 3 UAV, with comes with a FC6310 camera, equipped with a 1/2.3 inch CMOS sensor in this study. The sensor has a maximum resolution of 12.76 megapixels and a camera resolution of 2992 · 3992 pixels. The UAV operate automatically, from take-off to landing. The programming was performed using with the Drone Harmony app. All images were captured at nadir, i.e. perpendicular (90° ± 0.02°) to the ground surface, to facilitate surface calculations. Each flight lasted approximately ten minutes. The UAV imagery analysis involved coverage detection of water hyacinths. The pixel area had to be converted to real-ground area, by calculating the ground sampling distance (d_g) [m/pixels], as follows:

$$d_g = \frac{S_w \cdot H_f}{F_l \cdot w_i} \tag{A.1}$$

Here, S_w is the sensor width of the camera [m], H_f is the flight height [m], F_l is the focal length of the camera [m] and w_i is the image width [pixels]. All variables employed in the camera remained unchanged and the flight height was set at 10 m. A d_g value of $3.8 \cdot 10^{-3}$ m/pixel was found.

Water hyacinth and plastic detection using UAV imagery analysis

In this section, we detail the processing steps taken for both water hyacinth and plastic detection (Fig. S6). The choice in setting RGB threshold values was determined through trial and errors over a subset of the imagery dataset. For the water hyacinth detection, the same threshold values were applied for all the analyzed images. For the detection of plastic, changes in brightness between images did not

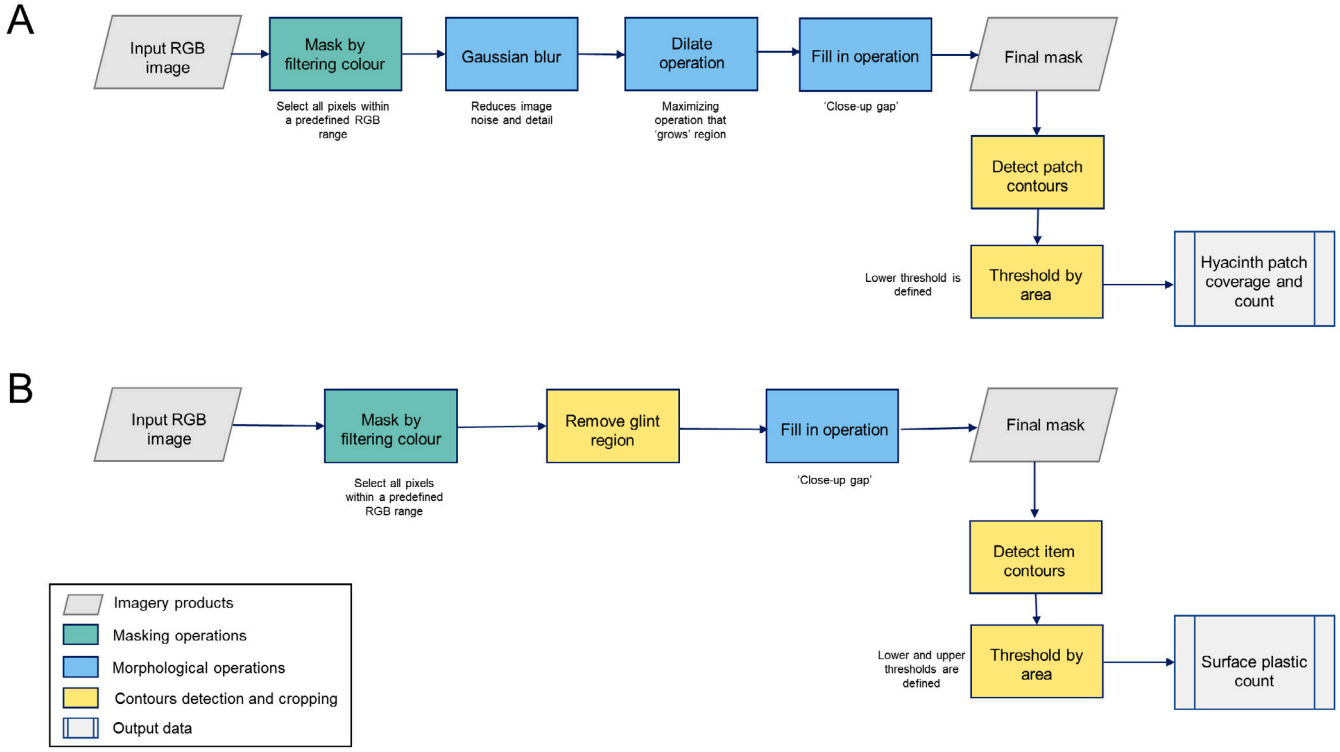

Fig. S6. Processing steps to detect: A. Water hyacinth patches and, B. Surface plastics.

allow us to use the same threshold values for the entire dataset. A few combinations were therefore retained and tested over batches of images (corresponding usually to the same measurement day). The best fitting threshold values were retained for the batch of images analyzed. For water hyacinth detection, images were then blurred with a Gaussian filter, to reduce noise. Noise in water hyacinth detection is the result of the configuration of patches. In general, patches were relatively loose (containing gaps and holes) with highly irregular edges. Various filter sizes were tested (see Sensitivity analysis in the Validation subsection). Ultimately, a filter size of 13 × 13 pixels was retained for the water hyacinth detection. No Gaussian blurring was necessary for the detection of plastic items, as the target objects are of relatively small size and the detection approach sought to maximize edge detection from the background elements rather than reduce noise. For water hyacinth detection, a dilate operation was necessary to reduce unnecessary details at the edges of patches. A final kernel size of 17 × 17 pixels was selected after trial and errors through visual inspection. A fill in (e.g.: binary closing) operation was performed for both detection approaches. This allows to fill in small gaps within the detected objects of interest. The closing was applied around a circle of a specified diameter [pixels]. A diameter of 10 pixels was chosen for both water hyacinth and plastic detection.

Sun glint and false positives with plastic detection

No distinct recurring sun glint shapes were found that could be used to filter out such areas on the UAV imagery dataset. We deemed it not feasible therefore to automatically detect sun glint and instead opted for manual removal of such areas. Cropping was therefore necessary to avoid false positive detection. Given that many images had a very large glint area, many were completely discarded for plastic detection (n = 1202). The cropping was performed on a batch basis. In images taken during the same UAV flight and same overpass direction, the area covered by sun glint was generally located in the same region of the images.

Sensitivity analysis for water hyacinth detection

We explored the sensitivity of the output variables for water hyacinth abundance (water hyacinth coverage and count of patches) to variations in input parameters for the three morphological operations performed (Gaussian blur, dilate, and fill-in operations). The sensitivity analysis was performed over a representative subset of the imagery dataset (n = 156 images, 4% of the total number of images analyzed). We performed a Mood's median test to compare the median of the two datasets. The alpha risk value was set at 0.05. We found a p-value > 0.05 (p-value = 0.11), indicating that the null hypothesis was confirmed and no significant difference can be assumed between the two sample populations.

For each morphological parameter, we calculated the change in output values for the count of patches and mean and median coverage area [%], based upon changes in input parameters [%]. Changes in input parameters were computed for approximately −50, −30, −10, 10, 30 and 50%. Given that kernel sizes have to be odd numbers, small deviations from the above-mentioned changes in input were sometimes necessary to fulfill this requirement. Ultimately, we expressed the sensitivity in terms of slope factor [%], calculated as the ratio between the change of output and the change of input parameters:

$$s = \frac{c_o}{c_i} \tag{A.2}$$

Where c_o is the change in output parameter and c_i in input parameter. The sensitivity analysis results (Table S3) show that the dilate parameter was the most sensitive, with a higher dilate kernel leading to a lower number of patches and higher water hyacinth coverage.

Table S3
Sensitivity analysis for input parameters (morphological operations) in water hyacinth detection on UAV images. This table reports the slope factor s, expressed in %.

	Dilate	Gaussian	Closing
Water hyacinth patch	−54	−21	−5
Mean water hyacinth coverage	55	25	4
Median water hyacinth coverage	64	28	12

Assessment of plastic detection

We assessed the accuracy of our detection approach for surface plastics by manually labeling plastics on a subset of our dataset (n = 273, 10% of the image dataset used for plastic detection). This validation set of images was selected randomly, using a Python function. We again performed a Mood's median test to compare the median of the two datasets and test whether the validation set could be considered representative of the entire imagery dataset. We found a p-value > 0.05 (p-value = 0.22), indicating that the null hypothesis was confirmed and no significant difference could be assumed between the two sample populations.

We manually identified and counted all surface plastics, irrespective of their size, on the validation set. An accuracy ratio [-] a_r was computed for each image, as follows:

$$a_r = 1 - \frac{|c_d - c_m|}{c_m} \tag{A.3}$$

Here, c_d is the total number of surface plastics detected on a given image and c_m the total number of surface plastics manually labeled. The overall accuracy ratio [-] was computed as the mean of accuracy ratios per image. We found an overall accuracy ratio of 75%. The number of surface plastics was found to be exactly the same between the validation and our detection approaches for 52% of the images (n = 141). For 37% of the images (n = 102), the detection approach underestimated the number of surface plastics when compared with the manual labeling. Only for a minority of the images (11%, n = 31) did the detection approach overestimate the number of surface plastics.

Surface plastic transport estimates

The mean plastic transport observation F [#/h] for observation point i was calculated using:

$$F_i = \frac{N_{t,i} + N_{o,i}}{t_i} \tag{A.4}$$

Here, N_t is the count of plastics [#] *trapped* in water hyacinths and N_o count of *open water* plastics [#] for observation point i during observation t_i [hour], respectively. This distinction between trapped plastics and open water plastics enables one to calculate the ratio of trapped plastics over the total count of plastics, which is reported as a ratio [-]. The total surface plastic transport F_t [#/h] was calculated using the following equation:

$$F_t = \frac{1}{n} \cdot W \cdot \sum_{i=1}^{n} \frac{F_i}{w_i} \tag{A.5}$$

Where n is the total number of observation points, W the total river width [m] and w_i is the observation segment width [m] (van Emmerik et al., 2022). The observation track width w_i [m] was estimated to be 15 m.

Hydrological data

We extracted all available daily data on rainfall and freshwater discharge in the Saigon river for about a year (Dec. 2020–Jan. 2022), corresponding to the period for which the measurements of plastic transport, water hyacinth coverage and plastic concentrations were undertaken. Rainfall and freshwater discharge are openly and freely available on the website of the Ho Chi Minh City Irrigation Service Management company (http://www.dichvuthuyloi.com.vn/vn/tin-tuc/thong-tin-ve-tinh-hinh-dien-bien-khi-tuong-thuy-van-719/). We used the rainfall data measured at the Mac Dinh Chi station, located in the first district of Ho Chi Minh City (10° 47′03.1"N; longitude: 106° 41′56.4"E), as this is the closest rainfall measurement station to our measurement sites. River discharge is not measured within Ho Chi Minh City but is approximately 125 km upstream in the Tay Ninh province where measurements correspond to the Dau Tieng reservoir inflow into the Saigon river. Monthly cumulative rainfall [mm] and mean freshwater discharge [m^3/s] were calculated based on the above-mentioned rainfall and discharge data and are presented in Fig. S9 (Appendix B).

A.1. Statistical analysis

To test statistical differences between plastic concentrations, plastic length scales, and plastic distribution between images with water hyacinth presence and without, we used the Kruskal–Wallis test. Similarly, we tested statistical differences in plastic transport between dry (December to April) and wet seasons (May to November). The Kruskal–Wallis test does not assume a normal distribution of the data. Prior to this, we examined the normality assumption of the data using the Kolmogorov–Smirnov test. As most variables were not normally distributed, a non-parametric test was used. The distinction between wet and dry months follows (Nguyen et al., 2020), but alternative definitions exist, potentially impacting the findings on seasonality patterns.

Appendix B. Supplementary figures and tables

See Figs. S7–S9 and Tables S4–S6.

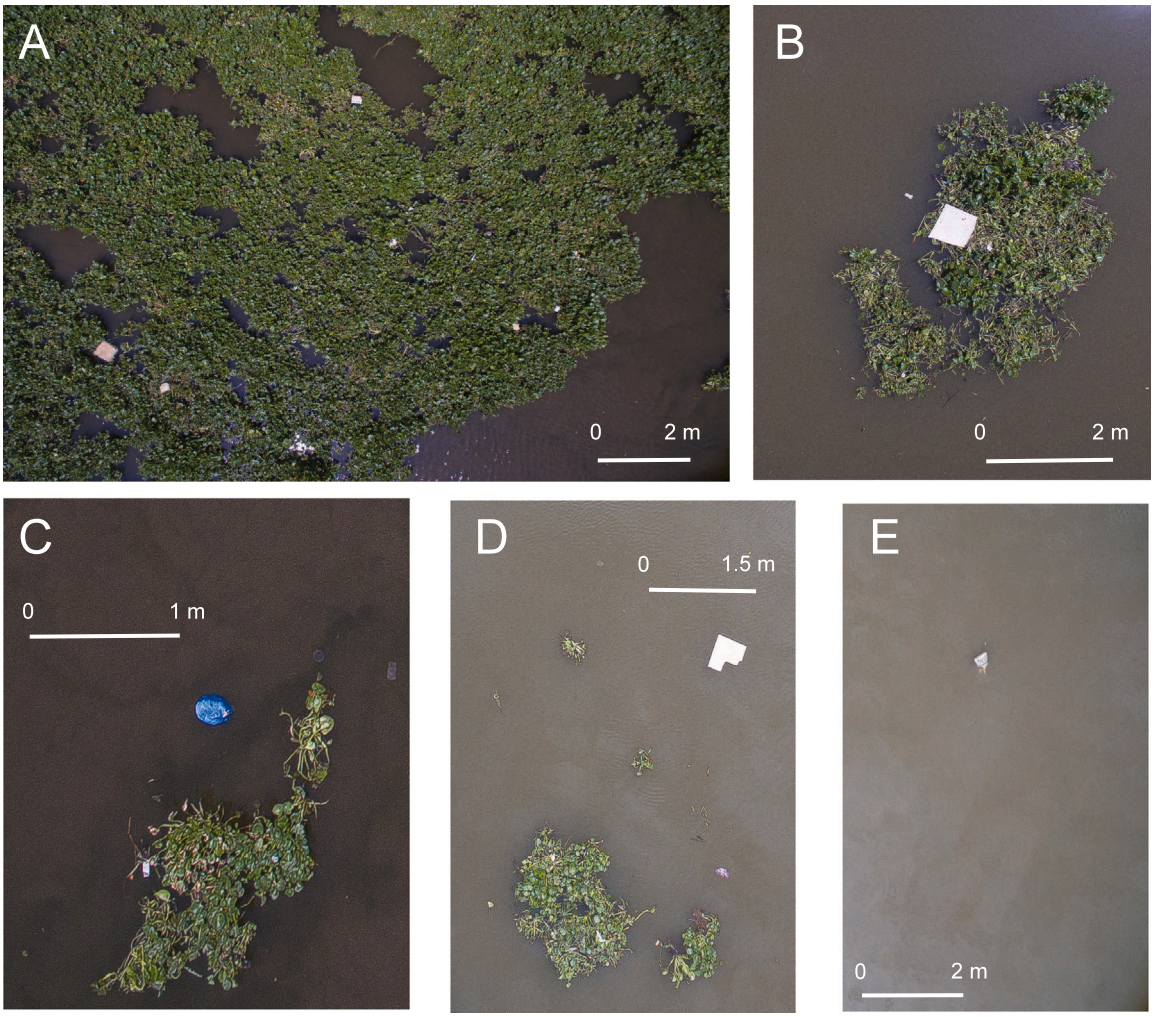

Fig. S7. Examples of water hyacinth patches, trapped and open water plastics from UAV images. A. Large water hyacinth patch occupying the entire UAV image area. B. Water hyacinth patch with large trapped plastic. C. Water hyacinth patch with large open water plastic next to it and smaller trapped plastic. D. Water hyacinth patches with large and small open water plastics next to them. E. Isolated open water plastic in open water river surface. Note that the UAV images have different spatial resolution, as some have been cropped to better enhance patch and plastic visibility.

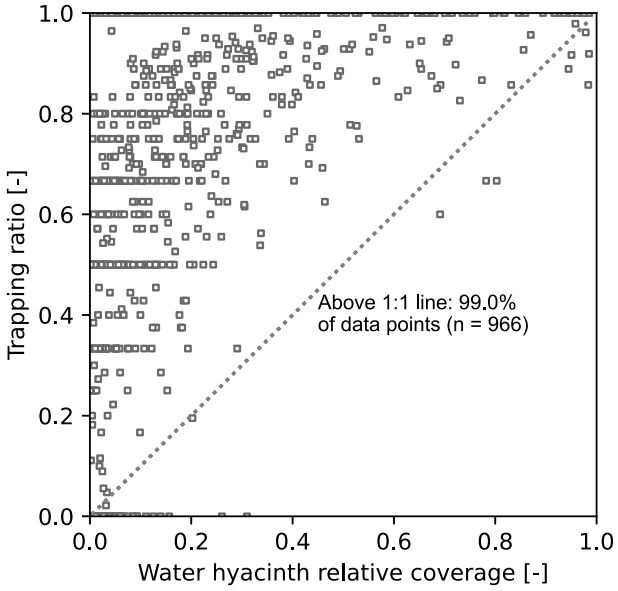

Fig. S8. Trapping ratio of plastics within water hyacinth patches vs water hyacinth relative coverage. Each data point corresponds to one UAV image for which both plastics and water hyacinths were present (n = 966). Trapping ratios can easily reach unity: even with low water hyacinth coverage, in the absence of open water plastics, all plastics become trapped. Moreover, trapping ratios often yield clear fractional values (0.50, 0.80, 0.66, 0.75), which reflects the method of calculation based on integers.

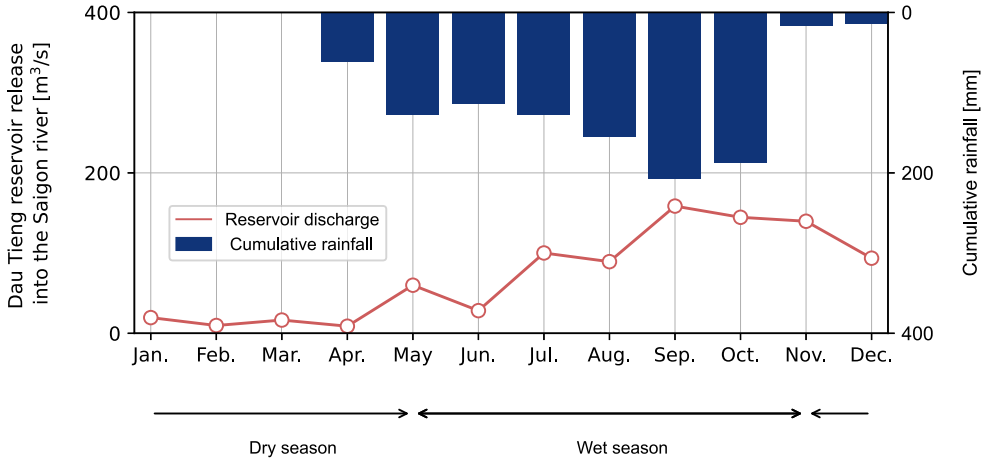

Fig. S9. Monthly rainfall and freshwater discharge at the Saigon river, for the year 2021. The rainfall data was monitored at the Mac Dĩnh Chi station in District 1, Ho Chi Minh City. The freshwater discharge (mean values) from the Dau Tieng reservoir into the Saigon river was measured at the Tây Ninh station.

Table S4
UAV images and plastic transport measurements per month. The values here refer to the total number of UAV images for water hyacinth abundance and plastic density. For plastic transport, the reported values correspond to the total number of observations from bridges. Blank cells indicate that no observations were conducted for that period. Months considered as part of the wet season are marked with an '*'.

	Number of measurements by month													
	Dec 20	Jan 21	Feb 21	Mar 21	Apr 21	May 21*	Jun 21*	Jul 21*	Aug 21*	Sep 21*	Oct 21*	Nov 21*	Dec 21	Jan 22
Plastic transport rates	54	108	72	126	126	90	54	36			18	90	90	36
Water hyacinth abundance	142	536	141	935		407	186					550	363	284
Plastic concentrations	105	388	108	391		376	95					435	192	274

Table S5
A. Plastic concentrations and; B. Water hyacinth distribution, plastic distribution and plastic length scale.

A. Plastic concentrations

	Items concentration [#/km^2]	Mass concentration [kg/km^2]	
		Mean mass	Median mass
Trapping concentration	$3.4 \cdot 10^5$	$3.4 \cdot 10^3$	$1.5 \cdot 10^3$
Open water concentration	$1.1 \cdot 10^4$	$1.1 \cdot 10^2$	$4.6 \cdot 10^1$
Total surface concentration	$3.0 \cdot 10^4$	$3.1 \cdot 10^2$	$1.3 \cdot 10^2$

B. Water hyacinth diameter & plastic length scale

Water hyacinth patch diameter [m]	No water hyacinth	0.4–1.0	1.0–5.0	5.0–10.0	Above 10.0
Mean patch diameter [m]	0.0	0.7	1.9	7.5	12.7
Patches distribution [%]	0	54	42	3	2
Patches with plastic [%]	0	26	73	79	87
Plastic distribution [%]	23	8	51	9	9
Trapping ratio [–]	0.0	0.5	0.8	0.9	1.0
Total surface plastic concentration [#/km^2]	$7.0 \cdot 10^3$	$4.4 \cdot 10^5$	$2.4 \cdot 10^5$	$1.8 \cdot 10^5$	$1.2 \cdot 10^5$
Average plastic length scale [m]	0.1	0.4	1.5	7.0	12.3

Table S6
Statistics on plastic transport, concentrations and hyacinth coverage in the dry and wet seasons.

Variables	Dry (Dec.–Apr.)	Wet (May–Nov.)	Statistical significance (p-value)
Plastic transport rates [#/h]	$1.4 \cdot 10^4$	$8.6 \cdot 10^3$	0.01
Trapped plastic concentrations [#/km^2]	$3.7 \cdot 10^5$	$2.8 \cdot 10^5$	<0.01
Open water plastic concentrations [#/km^2]	$1.3 \cdot 10^4$	$7.3 \cdot 10^3$	0.02
Total plastic surface concentrations [#/km^2]	$3.5 \cdot 10^4$	$2.3 \cdot 10^4$	<0.01
Water hyacinth coverage [–]	0.59	0.56	0.08
Average patch size [m^2]	2.7	2.3	0.08

Appendix C. Videos of plastic-water hyacinth interactions

The following UAV videos (10.4121/ec6776d7-1818-43a9-b88c-3d0fe26484c5) show plastic-water hyacinth interactions in the Saigon river, close to the measurement site, where UAV images were taken. Video 1 was taken at an elevation of 20 m and video 2 at 25 m.

References

Abd-Elaal, A., Mahmoud, A.A.H.M., 2022. Influence of water hyacinth on vertical velocity profile and drag coefficient in irrigation canals. J. Adv. Eng. Trends 41 (2).

Acha, E., Mianzan, H., Iribarne, O., Gagliardini, D., Lasta, C., Daleo, P., 2003. The role of the Rıo de la Plata bottom salinity front in accumulating debris. Mar. Pollut. Bull. 46 (2), 197–202.

Ballent, A., Pursuer, A., de Jesus Mendes, P., Pando, S., Thomsen, L., 2012. Physical transport properties of marine microplastic pollution. Biogeosci. Discuss. 9, 18755–18798.

Borrelle, S.B., Ringma, J., Law, K.L., Monnahan, C.C., Lebreton, L., McGivern, A., Murphy, E., Jambeck, J., Leonard, G.H., Hilleary, M.A., Eriksen, M., Possingham, H.P., Frond, H.D., Gerber, L.R., Polidoro, B., Tahir, A., Bernard, M., Mallos, N., Barnes, M., Rochman, C.M., 2020. Predicted growth in plastic waste exceeds efforts to mitigate plastic pollution. Science 369 (6510), 1515–1518. http://dx.doi.org/10.1126/science.aba3656.

Braudrick, C.A., 1997. Entrainment, Transport, and Deposition of Large Woody Debris In Streams: Results From a Series of Flume Experiments. Technical Report, Oregon State University.

Camenen, B., Gratiot, N., Cohard, J.-A., Tran, F., Nguyen, A.-T., Dramais, G., van Emmerik, T., Némery, J., 2021. Monitoring discharge in a tidal river using water level observations: Application to the Saigon River, Vietnam. Sci. Total Environ. 761.

Cook, C.D., 1996. Aquatic Plant Book. Balogh Scientific Books, p. 228.

Gasperi, J., Dris, R., Bonin, T., Rocher, V., Tassin, B., 2014. Assessment of floating plastic debris in surface water along the seine river. Environ. Pollut. 195, 163–166. http://dx.doi.org/10.1016/j.envpol.2014.09.001.

González-Fernández, D., Cózar, A., Hanke, G., Viejo, J., Morales-Caselles, C., Bakiu, R., Barceló, D., Bessa, F., Bruge, A., Cabrera, M., Castro-Jiménez, J., 2021. Floating macrolitter leaked from Europe into the ocean. Nature Sustain. 4 (6), 474–483.

González-Fernández, D., Hanke, G., 2017. Toward a harmonized approach for monitoring of riverine floating macro litter inputs to the marine environment. Front. Mar. Sci. 4, 86.

Hassan, A., Nawchoo, I.A., 2020. Impact of invasive plants in aquatic ecosystems. Bioremediation Biotechnol.: Sustain. Approaches Pollut. Degrad. 55–73.

Helinski, O.K., Poor, C.J., Wolfand, J.M., 2021. Ridding our rivers of plastic: A framework for plastic pollution capture device selection. Mar. Pollut. Bull. 165, 112095. http://dx.doi.org/10.1016/j.marpolbul.2021.112095.

Honig, B., 2020. Water hyacinth acts like 'plastic wrap' on the delta. https://www.fws.gov/story/2021-09/water-hyacinth-acts-plastic-wrap-delta/. (Accessed 14 March 2024).

Hurley, R., Braaten, H.F.V., Nizzetto, L., Steindal, E.H., Lin, Y., Clayer, F., van Emmerik, T., Buenaventura, N.T., Eidsvoll, D.P., kelsrud, A.O., Norling, M., Adam, H.N., Olsen, M., 2023. Measuring riverine macroplastic: Methods, harmonisation, and quality control. Water Res. 235, 119902. http://dx.doi.org/10.1016/j.watres.2023.119902.

Janssen, T.W., 2023. Floating Water Hyacinths Consistently Trap Surface Macroplastics Along the River Course. MSc thesis, Wageningen University and Research.

Janssens, N., Schreyers, L., Biermann, L., van der Ploeg, M., Bui, T.-K.L., van Emmerik, T., 2022. Rivers running green: water hyacinth invasion monitored from space. Environ. Res. Lett. 17 (4), 1613.

Kleinschroth, F., Winton, R., Calamita, E., Niggemann, F., Botter, M., Wehrli, B., Ghazoul, J., 2021. Living with floating vegetation invasions. Ambio 50, 125–137.

Koncki, N.G., Aronson, M.F., 2015. Invasion risk in a warmer world: modeling range expansion and habitat preferences of three nonnative aquatic invasive plants. Invasive Plant Sci. Manag. 8 (4), 436–449.

Ledieu, L., Tramoy, R., Mabilais, D., Ricordel, S., Verdier, L., Tassin, B., Gasperi, J., 2022. Macroplastic transfer dynamics in the loire estuary: Similarities and specificities with macrotidal estuaries. Mar. Pollut. Bull. 182.

Liro, M., Mikuś, P., Wyżga, B., 2022. First insight into the macroplastic storage in a mountain river: The role of in-river vegetation cover, wood jams and channel morphology. Sci. Total Environ. 838, 156354.

Lotcheris, R., Schreyers, L., Bui, T., Thi, K., Nguyen, H.Q., Vermeulen, B., van Emmerik, T., 2024. Plastic does not simply flow into the sea: River transport

dynamics affected by tides and floating plants. Environ. Pollut. 345, 123524. http://dx.doi.org/10.1016/j.envpol.2024.123524.

Meijer, L.J., van Emmerik, T., van der Ent, R., Schmidt, C., Lebreton, L., 2021. More than 1000 rivers account for 80% of global riverine plastic emissions into the ocean. Sci. Adv. 7 (18), eaaz5803.

Nguyen, T., Némery, J., Gratiot, N., Garnier, J., Strady, E., Nguyen, P.D., Tran, V., Nguyen, A., S. Tung Cao, S., Huynh, T., 2020. Nutrient budgets in the Saigon–Dongnai river basin: Past to future inputs from the developing Ho Chi Minh megacity (Vietnam). River Res. Appl. 36 (6), 974–990.

Pajai, W., 2022. Plastic river: Following the waste that's choking the Chao Phraya — thethirdpole.net. https://www.thethirdpole.net/en/pollution/plastic-river-following-waste-choking-chao-phraya/. (Accessed 14 March 2024).

Pritasari Arumdati, K., 2021. Hidden secrets of the water hyacinth and the guardians of the citarum river - clean currents coalition — cleancurrentscoalition.org. https://cleancurrentscoalition.org/hidden-secrets-of-the-water-hyacinth-and-the-guardians-of-the-citarum-river/. (Accessed 14 March 2024).

Reddy, K., Sutton, D., 1984. Water hyacinths for water quality improvement and biomass production. J. Environ. Qual. 13 (1), 1–8. http://dx.doi.org/10.2134/jeq1984.00472425001300010001x.

Rojas-Sandoval, J., Acedevo-Rodríguez, P., 2022. Eichhornia crassipes (water hyacinth). CABI Compendium http://dx.doi.org/10.1079/cabicompendium.20544, https://doi.org/10.1079/cabicompendium.20544.

Schreyers, L., van Emmerik, T., Biermann, L., van der Ploeg, M., 2022. Direct and indirect river plastic detection from space. In: IGARSS 2022-2022 IEEE International Geoscience and Remote Sensing Symposium. IEEE, pp. 5539–5542.

Schreyers, L., van Emmerik, T., Nguyen, T.L., Castrop, E., Phung, N.A., Kieu-Le, T.C., Strady, E., Biermann, L., van der Ploeg, M., 2021a. Plastic plants: The role of water hyacinths in plastic transport in tropical rivers. Front. Environ. Sci. 9, 686334.

Schreyers, L., van Emmerik, T., Nguyen, T.L., Phung, N.A., Kieu-Le, T.C., Castrop, E., L., B.T.-K., Strady, E., Kosten, S., Biermann, L., van der Berg, S., van der Ploeg, M., 2021b. A field guide for monitoring riverine macroplastic entrapment in water hyacinths. Front. Environ. Sci. 9, 716516.

The Ocean Cleanup, 2021. Interceptor 004: The first in the Caribbean | updates | the ocean cleanup — theoceancleanup.com. https://theoceancleanup.com/updates/interceptor-004-the-first-in-the-carribean/. (Accessed 14 March 2024).

Tramoy, R., Gasperi, J., Colasse, L., Silvestre, M., Dubois, P., Noûs, C., Tassin, B., 2020. Transfer dynamics of macroplastics in estuaries – New insights from the Seine estuary: Part 2. Short-term dynamics based on GPS-trackers. Mar. Pollut. Bull. 160, 111566. http://dx.doi.org/10.1016/j.marpolbul.2020.111566, Publisher: Elsevier BV.

Valero, D., Belay, B.S., Moreno-Rodenas, A., Kramer, M., Franca, M.J., 2022. The key role of surface tension in the transport and quantification of plastic pollution in rivers. Water Res. 226, 119078. http://dx.doi.org/10.1016/j.watres.2022.119078.

van Calcar, C.J., van Emmerik, T.H., 2019. Abundance of plastic debris across European and Asian rivers. Environ. Res. Lett. 14 (12), 124051.

van Emmerik, T., de Lange, S., Frings, R., Schreyers, L., Aalderink, H., Leusink, J., Begemann, F., Hamers, E., Hauk, R., Janssens, N., et al., 2022. Hydrology as a driver of floating river plastic transport. Earth's Future 10 (8), e2022EF002811.

van Emmerik, T.H., Frings, R.M., Schreyers, L.J., Hauk, R., de Lange, S.I., Mellink, Y.A., 2023a. River plastic transport and deposition amplified by extreme flood. Nature Water 1 (6), 514–522.

van Emmerik, T., Kieu-Le, T.C., Loozen, M., van Oeveren, K., Strady, E., Bui, X.T., Egger, M., Gasperi, J., Lebreton, L., Nguyen, P.D., et al., 2018. A methodology to characterize riverine macroplastic emission into the ocean. Front. Mar. Sci. 5, 372.

van Emmerik, T.H.M., Schreyers, L.J., Mellink, Y., Sok, T., Arias, M., 2023b. Large variation in Mekong river plastic transport between wet and dry season. Front. Environ. Sci. 11, http://dx.doi.org/10.3389/fenvs.2023.1173946, p.1173946.

van Emmerik, T., Strady, E., Kieu-Le, T.C., Nguyen, L., Gratiot, N., 2019. Seasonality of riverine macroplastic transport. Sci. Rep. 9 (1), 1–9.

Vriend, P., Schoor, M., Rus, M., Oswald, S.B., Collas, F.P., 2023. Macroplastic concentrations in the water column of the river rhine increase with higher discharge. Sci. Total Environ. 900, 165716. http://dx.doi.org/10.1016/j.scitotenv.2023.165716.